

## LOW RESISTIVITY OF Cu AND Fe DOPED PbS THIN FILMS PREPARED USING DC SPUTTERING TECHNIQUE

H. SOETEDJO<sup>a,b,\*</sup>, B. SISWANTO<sup>c</sup>, I. AZIZ<sup>c</sup>, S. SUDJATMOKO<sup>c</sup>

<sup>a</sup>*Study Program of Physics (Metrology-Electronics Material-Instrumentations), FMIPA, University of Ahmad Dahlan, Jalan Prof. Dr. Soepomo, S.H., Yogyakarta 55164, Indonesia.*

<sup>b</sup>*CIRNOV, University of Ahmad Dahlan, Jalan Cendana No 9A, Semaki, Yogyakarta 55166, Indonesia.*

<sup>c</sup>*PSTA – BATAN, Jalan Babarsari, Kotak Pos 6010, Yogyakarta 55281, Indonesia.*

Robust Cu-doped PbS (Lead Sulphide) thin films have been prepared using a dc sputtering technique. The PbS thin film deposition was characterized the crystal structure using XRD technique and also morphological surface using SEM-EDX. From the XRD measurement, Bragg peaks found are attributed to diffraction planes of the related material. The doping method was done by providing Cu plate directly on the plate surface of PbS target. This was also prepared for Fe-doped PbS thin film. The electrical property of Cu- and Fe-doped PbS thin films has been characterized using a Four-Point Probe technique. The resistivity was found to decrease rapidly from 189.4  $\Omega\text{cm}$  (un-doped) to 2.79  $\Omega\text{cm}$  (doped) for Cu, and decrease to 6.47  $\Omega\text{cm}$  for Fe (doped), respectively. The doping method is considerably novel. Texture Coefficient for (111) and (200) directions has also been calculated to support the correlation between diameter of Cu dopant plate and Cu concentration in PbS thin films.

(Received March 19, 2017; Accepted June 16, 2017)

*Keywords* : Lead Sulphide, sputtering, resistivity, semiconductor, infrared

### 1. Introduction

Lead Sulphide (PbS) is an IV-VI group semiconductor material with a direct and narrow bandgap of about 0.41 eV at room temperature has been studied widely due to its potential applications in various devices [1]. PbS material is a well-known material that plays an important role in optoelectronic device fabrications. This semiconductor material shows appropriate performance to absorb short wavelength infrared light spectrum. Use of PbS thin films as an IR sensor device is of interest for environment surveillance and military use. PbS has a high absorbance in NIR spectrum and has a great potential for IR photodetectors. This material is also extensively studied for solar cell devices because of its suitability in optical properties for that device design. PbS material has a cubic crystal structure with an absorption range in 1 – 3  $\mu\text{m}$  [2].

Various techniques have been used to deposit PbS thin film such of Chemical Bath Deposition (CBD) that is considerably less expensive, easy to handle and possible for large area deposition [3-5]. By using this technique PbS films were also doped using some metal dopants to exploit any changes of electrical properties of film materials. Dopant introduced to PbS thin film deposition is aimed to improve its electrical conductivity or resistivity. The increase of conductivity will be encouraging of the sensor device such of PbS material used for infrared sensors. Various metals doping has been introduced to PbS thin film such of Cu using CBD technique for electrical properties studies [6], also for investigation of material nanostructure [7]. In another work, PbS films have been doped using Zn [8] that was claimed for the first time prepared using CBD technique. They study photoluminescence properties from the thin film

---

\*Corresponding author: superadmin@cirnov.uad.ac.id

deposition. Another work was reported for Sr-doped PbS film by investigating the effect of doping concentration to the structural, morphological and optical properties of the material [9]. The above investigation was also carried out by using SILAR method for Ba-doped PbS thin film [10]. The results show that those properties directly depend on the Ba doping ratio.

For the purpose of physical properties improvement, Cu-doped PbS thin films have been explored by using various deposition techniques. By using a common CBD technique, several research works have been reported [6-8], and using a sputtering technique that material was also successfully deposited [13]. In the electrical property characterization, previous interesting work on Cu-doped PbS thin film has been reported by Zheng et al, 2016 [6]. From work, their results show that low resistivity has been achieved of the film by introducing various Cu concentrations. The resistivity was observed to decrease followed by the increase of doping concentration until achieving minimum value and then increase again. By using the same technique, Taouti et al, 2016 [13] were also reported the similar low resistivity. The trend of graph between resistivity and doping concentration is also observed. They studied further to the texture coefficient caused by thin film growth during the deposition. This texture coefficient seems interesting as we can see any strong correlation between the trend of the texture coefficient and the concentration of Cu introduced to the PbS films.

Another deposition technique of sputtering is also possible to prepare Cu-doped PbS thin film. Now days, by using this technique, there is very limited number of research works published particularly for this material. The sputtering technique offers a robust deposition beside any advantages of the quality of deposition process as this technique is run under vacuum chamber. Work has been reported using PbS material such of preparation of PbS nanocrystal-doped SiO<sub>2</sub> thin film [11]. They studied the structure properties of the material using XPS (X-Ray Photoelectron Spectroscopy) encompassing the Pb-S and Pb-O bonding under sputtering effect. Meanwhile, Bi-doped PbS quantum dot has been prepared to enhance robust photovoltaic devices based on an homojunction device to find power conversion efficiency [12].

In the present study, a thin film of PbS material used for a dc sputtering technique by introducing Cu-and Fe-doped PbS thin films is considerably novel and challenging. Use of sputtering technique in the vacuum chamber may introduce more purity of elements involved in the deposition process, also robust and short deposition time. Meanwhile, for doping technique, the doping material was put directly on the center of target material of PbS on the stage in the vacuum chamber. In our best knowledge, no research work reported previously in the preparation of metal doped PbS thin film using a sputtering technique. This new method to introduce doping leads any study of optimum resistivity of doping concentration. The correlation between the diameter of Cu and texture coefficient will be reported.

## **2. Material and measurement technique**

### **2.1 Material Preparation**

PbS sputter material target (99.9 % purity) has been ordered from QS Rare Element (New York, US) for 2" diameter and 0.125" thickness. The material was used directly prior the experiment. For the sputtering machine operation, the chamber was pumped using a rotary pump, later on, proceeded with diffusion pump until the pressure achieved in order of 10<sup>-5</sup> Torr. During the sputtering proces to introduce glow discharge, an argon gas was flown into the chamber. In this condition, the vacuum pressure was of 10<sup>-2</sup> Torr. For the initial investigation of the properties of PbS layer deposition, the substrate of microscope slide glass was used. Prior to the deposition, the microscope glass was used as a substrate and cleaned using alcohol under an ultrasonic cleaner. The area of substrate was 1.0 x 2.5 cm<sup>2</sup>. Stage of the target (cathode) was adjusted on the bottom in the chamber. This adjustment is aimed to minimize any contaminants deposit on the PbS film during the process.

The deposition was set at a deposition time of 30 minutes. In this experiment, the voltage applied was set at 1 kV and current of 10 mA, meanwhile the distance between target and substrate was 3.0 cm. This distance is assumed to be optimal for sputtering process done. Longer distance

has been introduced for this set up that could reduce the strength of deposition, while shorter distance could experience the implanting mechanism to the film material.

## 2.2 Doping Process

Doping was carried out using Cu material. This was done by introducing Cu plate (GoodFellow, 99.99 % purity, 0.5 mm thickness) directly on the surface of PbS target in the vacuum chamber. In the experiment, the diameter of Cu used was of 2.5, 5.0, 10.0, and 15.0 mm, respectively. Meanwhile, for Fe material (GoodFellow, 99.99% purity, 1.0 mm thickness), the diameter was 30.0 mm. For the doping mechanism, Cu plate was put in the center of the target to allow the optimum area during the sputtering process. Bigger diameter of the plate is assumed to provide higher doping concentration in the PbS thin film.

## 3. Thin film deposition Characterizations

### 3.1 X-ray Diffraction

The sample was characterized using XRD (RIGAKU Miniflex600) with  $\text{CuK}_\alpha$  radiation source ( $\lambda = 1.54 \text{ \AA}$ ) operated at room temperature. The samples were run by employing the incident angles ( $2\theta$ ) from  $2.0^\circ$  to  $80.0^\circ$  (angle resolution of  $0.02^\circ$ ).

### 3.2 SEM EDX

PbS thin film was characterized using SEM EDX (JED-2300, JEOL) to study surface morphology. From the observation many information regarding crystal grain size, boundary, and thin film homogeneity will be obtained. Meanwhile, EDX (Energy Dispersive X-ray) spectra were used to analyze the compositional of PbS films.

### 3.3 Four Point Probe

A Four Point Probe technique (VECCO, FPP 5000) was also used to investigate the electrical resistivity of the samples. The measurement was run for doped and un-doped PbS thin films to be studied their effects on resistivity due to the doping material. The layer thickness was also obtained from the calculation and found from the measurement.

## 4. Results and discussion

### 4.1 Structure of PbS thin film

PbS thin film deposition (for a deposition time of 30 minutes) has been characterized its structure using XRD. From the measurement XRD pattern obtained is shown in Fig. 1. Bragg peaks occur at angles ( $2\theta$ ) have been confirmed by comparing with X-ray diffraction powder database (JCPDS-ICDD, Card No 05-0592). From the comparison, it was concluded that Bragg angles approach to the database mentioned above at several angles given in Table 1. Narrow and sharp peaks indicate that PbS film deposited on a glass substrate is well crystallized. PbS has a cubic crystalline structure with a lattice constant of  $5.936 \text{ \AA}$ . By referring to the cubic structure, the calculation could be done to determine diffraction plane and  $d$ -spacing,  $d$  follows the formula below [14]:

$$d = \frac{a}{\sqrt{h^2 + k^2 + l^2}} \quad (1)$$

where,  $a$  is lattice constant of PbS (in  $\text{\AA}$ );  $h$ ,  $k$ , and  $l$  are Miller indices, respectively.

As PbS thin film was deposited on the substrate of glass, some Bragg peaks observed associated with this material ( $\text{SiO}_2$ ) was done by referring to JCPDS-ICDD, Card No 45-0130. The crystalline plane was determined by using a calculation based on the above equation as tabulated in Table 1.

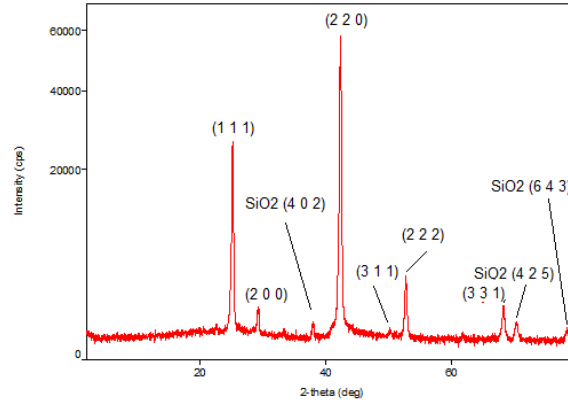


Fig 1. XRD pattern obtained from the measurement for PbS thin film deposition.

Table 1. List of peaks found from the experiment and calculated values.

No.	2-theta(deg) observed	d spacing (Å) observed	Intensities observed (cps)	<i>h k l</i> calculated	d spacing (Å) calculated
1	25.184(4)	3.53	17766(385)	1 1 1	3.43
2	29.226(18)	3.05	718(77)	2 0 0	2.97
3	37.93(2)	2.37	347(54)	4 0 2 (SiO <sub>2</sub> )	
4	42.290(3)	2.13	41666(589)	2 2 0	2.10
5	50.19(6)	1.81	131(33)	3 1 1	1.79
6	52.687(11)	1.73	2712(150)	2 2 2	1.71
7	68.16(3)	1.37	932(88)	3 3 1	1.36
8	70.23(4)	1.34	363(55)	4 2 5 (SiO <sub>2</sub> )	
9	78.27(7)	1.22	217(42)	6 4 3 (SiO <sub>2</sub> )	

By referring to the Bragg peaks indexing, crystalline grain size of PbS molecule,  $D$  could be calculated using the formula of Scherrer [15]:

$$D = \frac{K \lambda}{\beta \cos \theta} \quad (2)$$

Where,  $K$  is a constant ( $= 0.94$ ),  $\lambda$  is wavelength of X-ray radiation ( $\text{CuK}\alpha = 0.154 \text{ nm}$ ),  $\theta$  is Bragg angle ( $= 25.18^\circ$ ), and  $\beta$  is FWHM (Full Width at Half Maximum) of Bragg peak corresponds to plane of (111)  $= 0.260^\circ$ . From the calculation,  $D$  is found to be 35.26 nm. The size of crystal grain and its boundary may show the magnitude of conductivity or resistivity of thin film material. From SEM micrograph as shown in Fig. 2 for 20,000 times magnification, the surface morphology of PbS thin film (deposited for 30 minutes) is smooth, homogenous with very well-defined grain boundaries. The grain spread over the surface of substrate owing to the grain size in tens of nanometer that close to the calculation found of 35 nm. The result shows very sharp Bragg peaks observed as indicated by a narrow FWHM. This result also approaches the size reported by Palomino-Merino et al, 2014 [7] for a grain size of 37 nm as they prepared using a CBD technique.

Meanwhile, from EDX result for PbS thin film (as shown in Fig. 3), the percentages of atoms of Pb and S obtained are 57.10% and 42.90%, respectively. These results support the evidence that the thin film deposition consists of PbS material. As the sputtering technique is run under high vacuum chamber, it is found that no contaminant materials exist in the material composition. This environment is an advantage for thin film technology that requires high purity of material used.

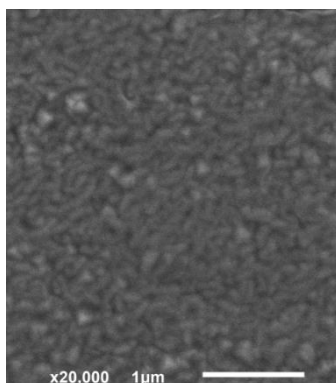


Fig 2. SEM Image of PbS thin film deposition.

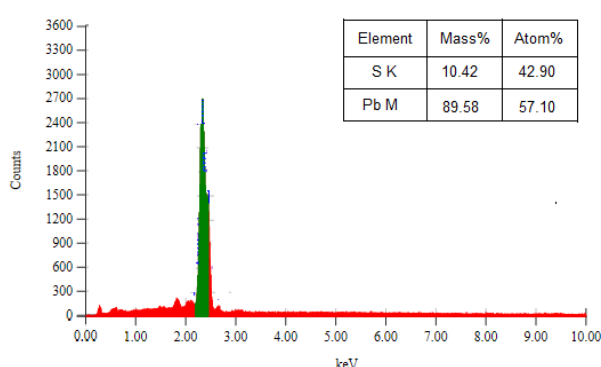


Fig 3. EDX spectrum of PbS thin film.

A comparison was made of the different structures of undoped PbS film, Cu-doped PbS film and Fe-doped PbS film, respectively. XRD measurement was carried out to these materials and the results are given in Fig. 4 by suppressing some curves allowing to see more clear different peaks position. From that figure, Bragg peak appears at angles of  $26.58^\circ$  is attributed to CuS (100) crystal. This angle is also observed for Cu-doped PbS prepared using CBD [13]. For Fe-doped PbS thin film, Bragg peak observed at angle of  $30.59^\circ$  is attributed to FeS (004) from dopant material (JCPDS-ICDD, Card No 24-0080). By referring to the XRD pattern, Cu-doped PbS thin film is found to be sharp and narrow spectra compare than that of the Fe-doped PbS thin film observed. This phenomenon shows that the atomic arrangement of Cu dopant in PbS molecules has a better crystallinity.

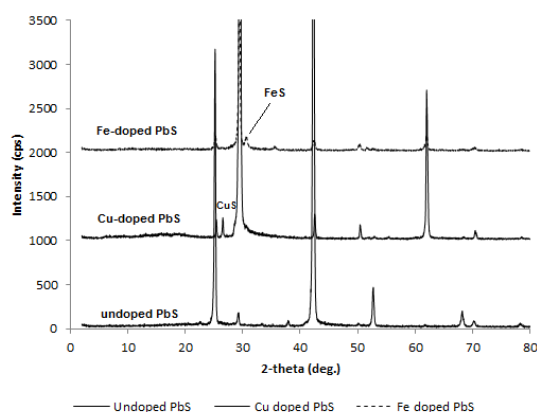


Fig. 4. XRD patterns for Cu- and Fe-doped PbS thin films.

XRD measurement was also run for various diameters of Cu dopant plate into PbS thin film as the results are shown in Fig. 5. From the figure, the increase of doping concentration (diameter of the dopant plate) will change the Bragg peaks intensities. The change shows a variation among the Bragg peaks that is due to the degree of crystallinity respects to the diffraction plane. By investigating diffraction plane (111) and (200) for all materials as given in Fig. 6, the variation of diffraction planes depend on the growth orientation during the deposition that will be explained later.

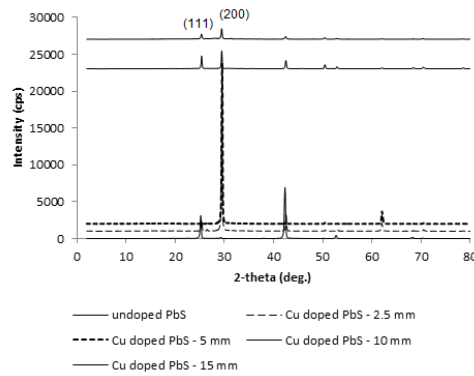


Fig. 5. XRD patterns for various doping concentrations (various diameters of Cu plate) introduced to PbS thin films.

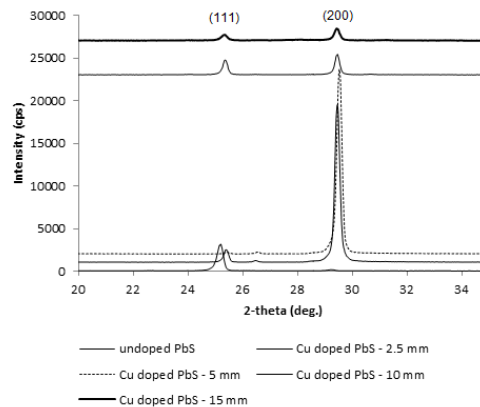


Fig. 6. XRD patterns for various doping concentrations (various diameters of Cu plate) at selected angles of (111) and (200) planes.

Electrical sheet resistivity was also measured using a Four Point Probe technique. By introducing Cu plate on the target material for various diameters of 2.5 to 20.0 mm the resistivity was observed to decrease until achieving the minimum value (at a diameter of 5.0 mm), then increase again (Fig. 7). Nevertheless, the resistivity of Cu-doped PbS decreases drastically from 189.4  $\Omega\text{cm}$  (un-doped) to 2.79  $\Omega\text{cm}$ . The values obtained are uniform over the surface of samples. This phenomenon exhibits the doping method was done in the good process. The rapid decrease of resistivity above shows the comparable result obtained by using a CBD technique [6]. From their work, resistivity decreases by the increase of doping concentration up to 6.4 %, later on the values increase again. This trend is similar as we observed using a different technique of sputtering. Cu-doped PbS thin film we prepared is p-type due to the Pb ion vacancies. The increase of resistivity (increase the doping) after achieving the minimum value is assumed by the increase of scattering among the ions.

As the film deposited for the increase of diameter of Cu plate (Fig. 7), the film deposition thickness was measured (using a Four Point Probe) to increase initially after doping introduced to

PbS until achieving the maximum thickness at a diameter of 5 mm followed by the decrease of its thickness. This phenomenon may show that the grain size is bigger at the smaller diameter and then decrease by the increasing of the plate's diameter. Bigger grain size may affect to the decrease of the resistivity. All the samples were prepared at the same deposition time of 30 minutes and also the same environment. This mechanism allows the sputtering particles yield the same amount during the deposition. By varying the diameter of Cu dopant plate on the PbS plate target, the ion Cu doped in the PbS will occur proportionally. The weight of the material (PbS and Cu) after sputtering process will reduce because the volume of plate used (Cu and PbS) will reduce during the sputtering process and deposited over the area of the substrate's surface and also on the wall of vacuum chamber. Cu-doped PbS thin film prepared using a sputtering technique may introduce any advantages such of robust deposition that will become a critical requirement for the devices products. This technique also offers fewer contaminants during the process, and less time consuming for a deposition that needs about 10 – 30 minutes. This property seems different with other technique such of CBD that needs longer time for deposition and less robust for the film deposition. The same experiment using a sputtering technique was also run for Fe-doped PbS thin film, the results are given in Fig. 8. From that figure, it is observed that the increase of diameter of dopant plate will be followed by the decrease of resistivity until achieving the minimum value and then increase again.

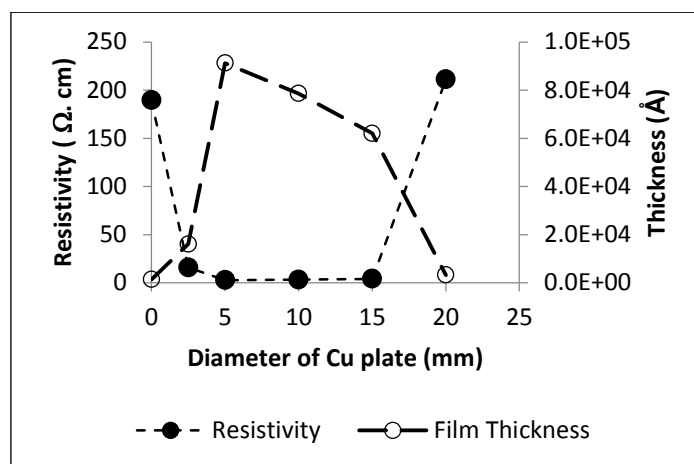


Fig 7. The relationship between the resistivity, film thickness and the diameter of Cu plate of Cu-doped PbS film deposition.

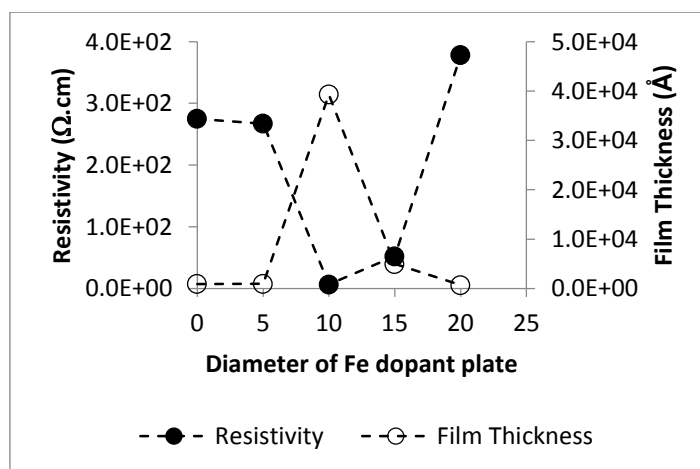


Fig 8. The relationship between, resistivity, film thickness and diameter of Fe plate for Fe-doped PbS thin film.

Texture Coefficient, TC as mentioned previously could be used to study the degree of preferred growth orientation of thin film through the following equation [13]:

$$TC = \frac{I(hkl)/I_0(hkl)}{\frac{1}{N} \sum N \left( \frac{I(hkl)}{I_0(hkl)} \right)} \quad (3)$$

Calculation of TC for (111) direction shows that the increase of doping plate diameter followed by the decrease of TC until achieving the minimum value and then increase again. This trend is assumed to be similar to what Touati et al, 2016 [13] reported the increase of Cu doping concentration and TC. Also, there is a similar trend of this curve for the relationship between doping concentration and resistivity they reported. In our measurement, from Fig. 9, the growth orientation of Cu-doped PbS thin film achieves the preferential orientation for (111) and (200) peaks after a concentration corresponds to the diameter of doping plate of 10 mm and higher. Both orientations show the increase of TC indicates that the thin film crystal structure prepared using a sputtering technique improve its quality. This phenomenon is considered to be superior to this technique as the increase of doping concentration of Cu introduced to the PbS film does not alter the crystal plane orientation too much. The robust property of thin film deposition may cause the structure can maintain the growth orientation that may be experienced by using other techniques.

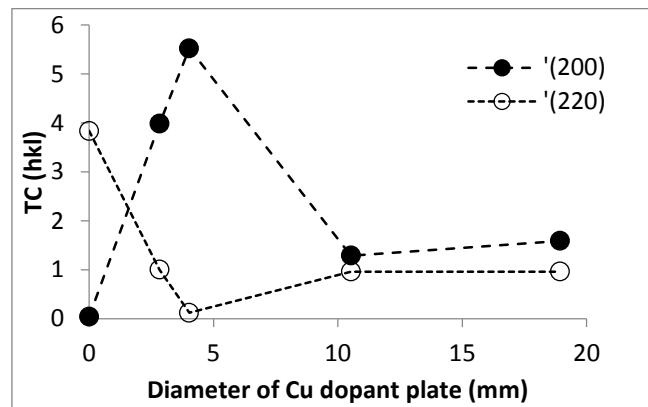


Fig. 9. Texture Coefficient (TC) for (111) and (200) directions in Cu-doped PbS thin films.

## 5. Conclusion

Cu- and Fe-doped PbS thin films have been successfully prepared using a dc sputtering technique. The new method of doping by introducing Cu and Fe plates directly on the sputtering target on the stage leads the interesting technique. Bragg peaks observed from the experiment support the evidence of the crystalline structure of PbS. Additional peaks of SiO<sub>2</sub> substrate were also determined. A significant decrease of resistivity was obtained to be 2.79 Ωcm when Cu-doped PbS introduced from undoped PbS of 189.4 Ωcm. This rapid decrease is comparable to what previously work observed using the same material but using a different technique of CBD. For Fe-doped PbS thin film, the lowest resistivity was found to be 6.47 Ωcm. Texture Coefficient (TC) calculated from Cu-doped PbS thin films shows a similar trend between doping concentration and resistivity that was considered to correlate with the diameter of doping plate used. The sputtering technique used by introducing doping method using metals of Cu and Fe to find a significant decrease of resistivity and robust films are encouraging.

## References

- [1] M. A. Barote, A. A. Yadav, T. V. Chavan, E. U. Masudar, *Digest J. Nanomat. Biostruct.* **6**(3), 979 (2011).
- [2] N. Choudhary, B. K. Sarma, *Bull. Mater. Sci.* **32**(1), 43 (2009).
- [3] S. Thirumavalava, K. Mani, S. Suresh. *J. Ovonic Res.* **11**(3), 123 (2015).
- [4] C. E. Pérez-García, R. Ramírez-Bon, Y. V. Vorobiev, *Chalcogen. Lett.* **12**(11), 579 (2015).
- [5] E. M. Nasir, M.M. Abbas. *Chalcogen. Lett.* **13**(6), 271 (2016).
- [6] X. Zheng, F. Gao, F. Ji, H. Wu, J. Zhang, X. Hu, Y. Xiang, *Mater. Lett.* **167**, 128 (2016).
- [7] R. Palomino-Merino, O. Palomino-Moreno, J.C. Flores-Garcia, J. Hernandez-Tecorralco, J. Martinez-Juarez, A. Moran-Torres, E. Rubio-Rosas, G. Hernandez-Tellez, R. Guitierrez-Perez, L.A. Chaltel-Lima, *J. Nanosci. Nanotechn.* **14**(7), 5414 (2014).
- [8] L.R. Singh, S.B. Singh, A. Rahman, *Chalcogen. Lett.* **10**(5), 167 (2013).
- [9] E. Yücel, Y. Yücel, *Ceramics Int.* **43**, 407 (2017).
- [10] Y. Gülen, *Acta Phys. Polonica A*, **126**(3), 763 (2014).
- [11] R. Reiche, R. Thielsch, S. Oswald, K. Wetzig, *J. Electr. Spectros. Related Phenom.* **104**, 161 (1999).
- [12] A. Stravinadis, A.K. Rath, F.P.G. de Arquer, S.L. Diedenhofen, C. Magén, L. Martinez, D. So, G. Konstantatos, *Nature Comm.* **1** (2013).
- [13] B. Touati, A. Gassoumi, I. Dobryden, M.M. Natile, A. Vomiero, N.K. Turki, *Superlattices and Microstruct.* **97**, 519 (2016).
- [14] B.D. Cullity, *Elements of X-Ray Diffraction* (3<sup>rd</sup> ed.), Prentice Hall, New Jersey (2001).
- [15] A.C. Bose, P. Thangadurai, S. Ramasamy, *Mater. Chem. Phys.* **9**, 72 (2006).